ORIGINAL ARTICLE

The characteristics of air pollutants during different seasons in the urban area of Lanzhou, Northwest China

Mikalai Filonchyk[1] · Haowen Yan[1]

Abstract

Based on data from ground-based air quality stations, space–time variations of six principal atmospheric pollutants, such as particulate matter ($PM_{2.5}$ and PM_{10}) and gas pollutants (SO_2, NO_2, CO, and O_3), obtained from January 1, 2014 to December 31, 2017 in the city of Lanzhou, have been studied. Average total concentrations of $PM_{2.5}$ and PM_{10} were 53.2 ± 26.91 and 124.54 ± 82.33 μg/m^3, respectively; however, the results showed that in 75.53% and 84.85% days, concentrations of these pollutants exceeded Chinese National Ambient Air Quality Standard and in 100% days exceeded World Health Organization guidelines standards. Daily mean values of aerosol optical depth and Ångström exponent based on data, received by satellite Moderate Resolution Imaging Spectroradiometer, show a broad range of values for aerosol optical depth (from 0.018 to 1.954) and Ångström exponent (from 0.003 to 1.8). Results of principal components analysis revealed three factor loadings. Thus, Factor 1 has the relevant loadings for $PM_{2.5}$, PM_{10}, CO, SO_2, and NO_2 (36%) and closely associated with transport emissions and industrial sources, which contribute to air pollution in Lanzhou. Factor 2 was heavily loaded with temperature and visibility (16.94%). Factor 3 consisted of relative humidity (14.11%). Cluster analysis revealed four subgroups: cluster 1 ($PM_{2.5}$, NO_2, SO_2), cluster 2 (CO), cluster 3 (PM_{10}) and cluster 4 (relative humidity, visibility, temperature, O_3, wind speed), which were compliant with results, obtained from principal components analysis. Positive correlation was found among all pollutants, other than O_3. According to processed backward trajectories obtained by Hybrid Single-Particle Lagrangian Integrated Trajectory model, it was found that movement of air masses occur from north, northwest, and west directions—the location of principal natural sources of aerosols.

Keywords Air pollution · Atmospheric pollutant · Principal component and cluster analysis · Urban area · Lanzhou

Introduction

Special attention to aerosol content and variation in atmosphere is caused by its ability to influence radiation processes with the relevant climatic and less major changes of temperature and humidity characteristics, visibility as well as business activity (Chan et al. 2002; Fang et al. 2017). Another reason of increased interest in aerosol pollution is relationship of a number of diseases with elevated level of particulate matter, which has a significant adverse effect not only on a human body, increasing the risk of cardiovascular

and respiratory diseases (Pan et al. 2010; Tao et al. 2014; Xia et al. 2017), but on the animal and the vegetable worlds as well (Costa and Dreher 1997). The findings of epidemiological studies were the basis for the World Health Organization (WHO) to enter into the list of pollutants required for air quality assessment, criteria such as particulate matter with aerodynamic diameter no more than 2.5 μm ($PM_{2.5}$) and no more than 10 μm (PM_{10}), as well as principal gas pollutants, such as nitrogen dioxide (NO_2), sulfur dioxide (SO_2), carbon monoxide (CO), and ozone (O_3), having established guidelines on air quality for $PM_{2.5}$ (10 μg/m^3 annual and 25 μg/m^3 24-h mean), PM_{10} (20 μg/m^3 annual and 50 μg/m^3 24-h mean), O_3 (100 μg/m^3 8-h mean), NO_2 (40 μg/m^3 annual and 200 μg/m^3 1-h mean), SO_2 (20 μg/m^3 24-h and 500 μg/m^3 10-min mean) (WHO 2005).

Intensive development of manufacturing industry, transport and power generating industry, observed in China, result in permanent increase in atmospheric pollutant emission.

✉ Haowen Yan
haowen2010@gmail.com

Mikalai Filonchyk
filonchyk.mikalai@gmail.com

[1] Department of GIS, Faculty of Geomatics, Lanzhou Jiaotong University, Lanzhou 730070, China

Therefore at present a routine observation for air pollution, which in 2017 was carried out on 1445 monitoring stations in 367 largest cities of China, combined into a single State Network of Air Quality Monitoring (http://datacenter.mep.gov.cn/), is the constituent part of environmental monitoring. Observations over pollutant concentrations are carried out according to uniform standards of the Ministry of Environmental Protection (MEP), based on annual, 24 h and hourly concentration values by each of the atmospheric pollutants. Currently relevant Chinese National Ambient Air Quality Standard (CNAAQS) GB3095-2012 (MEP 2012) includes two classes of limit values. Class 2 standards are applied to specific regions, such as national parks. Class 2 standards are applied to all other regions, including urban and industrial areas. 24 h mean concentrations for two classes are 35 and 75 $\mu g/m^3$ for $PM_{2.5}$, 50 and 150 $\mu g/m^3$ for PM_{10}, 50 and 150 $\mu g/m^3$ for SO_2, 80 $\mu g/m^3$ for NO_2, 4 mg/m^3 for CO and 1-h values O_3 are 160 and 200 $\mu g/m^3$, respectively.

Based on regular measurements, the monitoring network in China was involved in a number of investigations on $PM_{2.5}$, PM_{10}, related to short-term variability of their mass concentration and multiannual trends (Zheng et al. 2015; Filonchyk and Yan 2018), sources of generation (Hagler et al. 2006; Wang et al. 2013), mechanism of impact on human health (Tao et al. 2014). A significant place is held by descriptions of aerosol episodes in urban agglomerations, while the majority of authors try to establish the reasons of such episodes formation (Huang et al. 2011; Fang et al. 2017). A large amount of investigations were focused on the study of large megalopolises such as Beijing, Shanghai, Chengdu (Lv et al. 2015; Zhao et al. 2015; Zheng et al. 2015; Kong et al. 2016), or certain economically developed regions of the country (Hagler et al. 2006; Hu et al. 2014; Chen et al. 2017; Yan et al. 2018). Thus, investigations, carried out from April 2014 to April 2015 in 190 large cities of China, showed a mean concentration of $PM_{2.5}$ over the country as 57 ± 18 $\mu g/m^3$ (Zhang and Cao 2015). In Beijing in 2013 mean year concentrations of $PM_{2.5}$ were 102.1 ± 73.6 $\mu g/m^3$ (Xu et al. 2016a, b). Mean year concentrations of $PM_{2.5}$ and PM_{10} in Shenzhen in 2013 were 43 and 62 $\mu g/m^3$ (Xia et al. 2017); in Shanghai in 2013–2014—56.3 and 76 $\mu g/m^3$ (Xu et al. 2017); in Tianjin in 2014—106.7 and 156.2 $\mu g/m^3$, and in Jilin—96.9 and 137.2 $\mu g/m^3$ (Zhou et al. 2017); in Chengdu in 2014–2015—73, 64, 65 $\mu g/m^3$ and 112, 103, 105 $\mu g/m^3$ (Xiao et al. 2018); in Hangzhou in 2014–2017—55.4 and 84.7 $\mu g/m^3$ (Zheng et al. 2017), respectively.

Previous investigations, aimed at Lanzhou atmosphere study, showed that in the period from 2002 to 2008 annual mean value of PM_{10} concentration was 197 $\mu g/m^3$ (Na et al. 2013), in 2013 annual mean value of $PM_{2.5}$ was 66 $\mu g/m^3$ (Wang et al. 2014). Guan et al. (2017) studied seasonal concentrations of $PM_{2.5}$ and PM_{10} in 2014, which showed values 53 ± 21 and 145 ± 74 $\mu g/m^3$, 43 ± 12 and 93 ± 26 $\mu g/$ m^3, 55 ± 23 and 103 ± 37 $\mu g/m^3$, 82 ± 40 and 131 ± 42 $\mu g/m^3$, respectively, for spring, summer, autumn, and winter. In summer 2015, concentrations were 38.8 $\mu g/m^3$ for $PM_{2.5}$ and 98.8 $\mu g/m^3$ for PM_{10} (Filonchyk et al. 2016). And in the period 2014–2017 spring concentrations were 42.37 $\mu g/m^3$ for $PM_{2.5}$ and 138.15 $\mu g/m^3$ for PM_{10} (Filonchyk et al. 2018). The results obtained show that air quality problem is urgent for many Chinese cities, concentrations of atmospheric pollutants exceed not only CNAAQS, but also WHO guidelines on air quality.

However, even multibranch ground-based monitoring network may not always fully provide information required by nature protection services, as at some areas of the territory, ground-based monitoring is impossible due to various relief or geographical location of the monitoring area. Therefore the technology of spaceborne remote sensing by measuring aerosol optical depth (AOD) provides for cost-effective way of conducting epidemiological studies and atmosphere monitoring in various scales (Remer et al. 2005; Tsai et al. 2011).

Lanzhou is one of the largest industrial cities of Northwest China, surrounded by mountains and distant from sea, located in a unique arid region, and, under the influence of anthropogenic and natural factors, experiences serious atmospheric pollution. Previous investigations of Lanzhou atmosphere were predominantly aimed at the study of total content of particulate matter (Wang et al. 2009; Filonchyk et al. 2016, 2018) and chemical constituents in air basin of the city (Fan et al. 2014; Qiu et al. 2016; Tan et al. 2016), influence of meteorological and synoptical parameters on pollutant levels with use of data from ground-based stations (Zhao et al. 2013; Qiu et al. 2016) or data of satellite sounding (Xin et al. 2007; Cao et al. 2013). These circumstances as well as out-dated information have impelled to conduct investigations in an integrated fashion, with simultaneous use of data from ground-based stations and data of satellite sounding.

This investigation involves the use of daily data concerning six atmospheric pollutants ($PM_{2.5}$, PM_{10}, NO_2, SO_2, CO, and O_3) as well as data on AOD and AE in Lanzhou from January 1, 2014 to December 31, 2017, encompassing all seasons. Taking into account rapid changes in air pollution, it is necessary to determine characteristic temporal and spatial variations in pollutants as well as their connections with meteorological conditions and evaluate changes in air quality to develop preventive and control measures. To evaluate over-limits of standard levels and concentrations of pollutants, determine temporal and spatial characteristics of air pollutants concentrations, analyze interrelation between pollutants and meteorological factors, as well as determine the sources and ways of transportation of polluting air masses into city, the monitoring was conducted continuously on several areas over 4 years.

Materials and methods

Study area

Lanzhou is located in the catchment of the Yellow River and surrounded with mountains in the coordinates from 102°58′E to 104°57′E and from 35°58′N to 37°02′N with total area of 13,085.6 km². There are considerable differences in the city topography, which descends from the west to the east with the extension of urban area along the river from the north to the south over 60 km, with the average height 1572 m (Fig. 1). Typical climate characteristics of the city are low air humidity (annual mean relative humidity is 50–70%) and low wind speed (constant speed of dry wind is 1.78–3.57 m/s). Annual mean amount of precipitations is 327 mm, predominantly in June–September. Annual mean temperature is 10.3 °C, and average number of solar hours is 2446 h. During 2016 the headcount of Lanzhou resident population was 3.705 million (LSB 2018).

Data and processing

By the end of 2012 only three atmospheric pollutants (PM_{10}, SO_2, and NO_2) were monitored on a regular basis; however, starting from 2013, MEP began on-line publishing of information on hourly concentration of gases (SO_2, NO_2, CO, O_3) and particulate matter ($PM_{2.5}$ and PM_{10}). Quadrennial data were obtained form database of the Ministry of Environmental Protection of the People's Republic of China based on results, provided by four automated air quality stations, located in the urban area, which coordinates are shown in Fig. 1. Monitoring stations are located in the city so as to perform monitoring over air pollution in all city districts, where station S1 is located in industrial area with enterprises of various fields (production of mineral fertilizers, petroleum processing, cement production, and power plants), S2 is located in the transition zone from industry to residential quarters, S3 and S4 are located in residential quarters with high density of population and housing. These stations control mass concentration of pollutants in the air near the ground surface. Data on all pollutants from these stations involve hourly and 24 h mean values of mass concentrations. For measurement of SO_2,
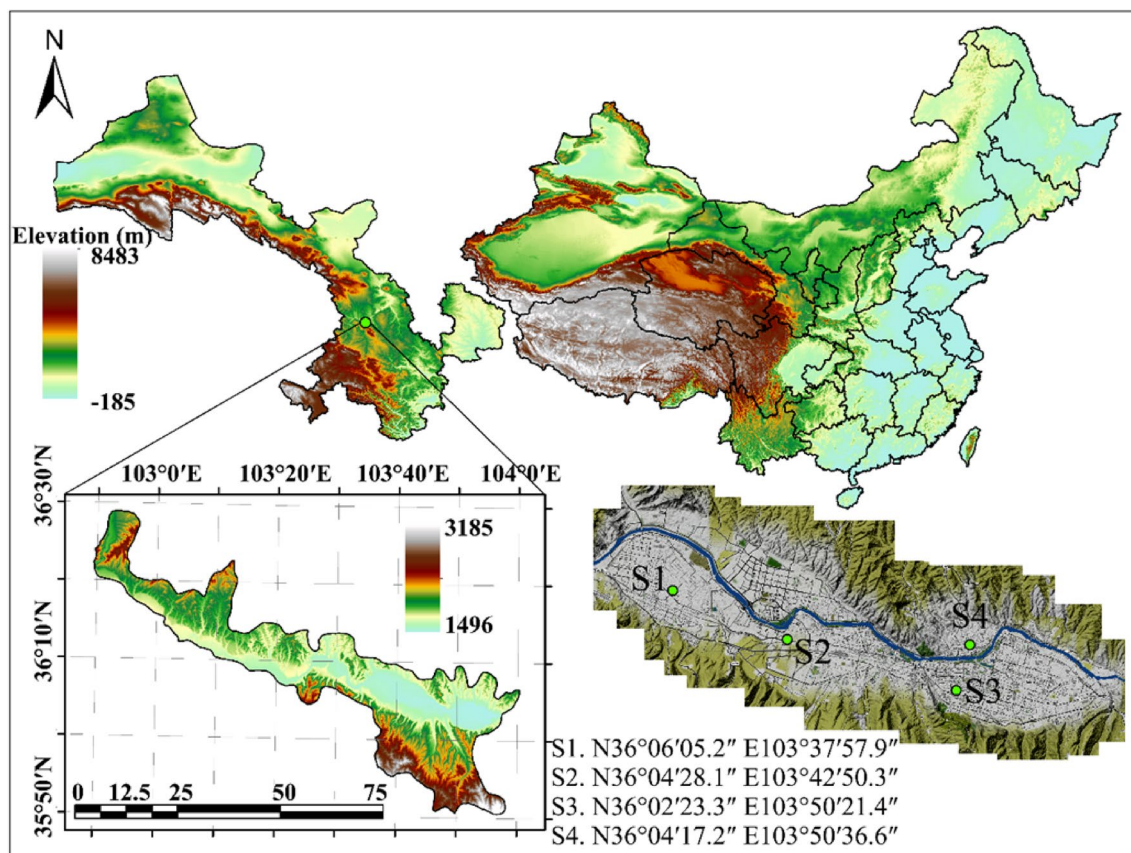

Fig. 1 Geographical location of study area as well as sampling sites in Lanzhou

NO_2, O_3, and CO concentrations all automated monitoring stations are based on China Environmental Protection Standards HJ 193–2013 (MEP 2013b), and $PM_{2.5}$ and PM_{10} according to China Environmental Protection Standards HJ 655–2013 (MEP 2013a).

Information on aerosols and their types was obtained using satellite data MODIS (Moderate Resolution Imaging Spectroradiometer) and CALIPSO (Cloud-Aerosol Lidar and Infrared Pathfinder Satellite Observations). MODIS, created by Santa Barbara Remote Sensing and launched by National Aeronautics and Space Administration (NASA), takes pictures in 36 spectral bands and has a wide area coverage (about 2330 km) and high temporal resolution (every 1–2 days). It is widely used to observe a global dynamics of the Earth (changes in cloud cover, radiation balance) and the processes, which occur in oceans, over land, and in the lower atmosphere layers. AOD represents the total column loading of aerosols in the atmosphere and is extracted as level 2 product at the temporal resolution 3 km (Remer et al. 2013). AOD is obtained using aerosol algorithm MODIS Terra (Collection 6.1) combined Dark Target and Deep Blue AOD at 550 nm (Sayer et al. 2014) from product MOD04_3K, obtained from Level-1 and Atmosphere Archive and Distribution System Distributed Active Archive Center (LAADS DAAC). Got off the ground in 2006 satellite CALIPSO is intended for the study of mutual influence of clouds and aerosols (particulate matter) on weather, climate and quality of aerial environment. Payload involves three tools: Cloud-Aerosol Lidar with Orthogonal Polarization (CALIOP), Wide-Field Camera (WFC) and Imaging Infrared Radiometer (IIR), which deal with search and study of aerosol particles in the Earth atmosphere and may distinguish aerosol particles from particles, composing clouds, as well as give information on aerosols types classification and their vertical distribution in atmosphere (Winker et al. 2009, 2010).

Data of ground meteorological parameters, including surface wind speed (WS, w/s), surface air temperature (T, °C), horizontal visibility (V, km), relative humidity (RH, %) and amount of precipitations (AP, mm), were obtained from meteorological stations in Lanzhou and Gaolan. According to data of ground changes in atmospheric pollutants, data of meteorological parameters, presented by Gansu Meteorological Bureau, also include all days of investigation from January 1, 2014 to December 31, 2017.

In view of the fact that satellite MODIS Terra crosses the Line at 10.30 LST (local solar time), it was decided to regard this time as a daily mean by AOD. In order for data on PM concentration and meteorological parameters from ground observations over air quality were in line with MODIS data, 2 h mean value from 10.00 a.m. to 12:00 p.m. was chosen (LST) (which corresponds the time of satellite interception).

Results and discussion

Total content and year-to-year variations of pollutants in the city atmosphere

Based on data received from four air quality stations, located in Laznhou, and consisting of 1460 days of samplings, annual and daily mean concentrations of pollutants ($PM_{2.5}$, PM_{10}, SO_2, NO_2, O_3, and CO) were defined, and evaluation of pollutants, exceeding standard levels, was performed.

Table 1 and Fig. 2 show annual averaged concentrations of $PM_{2.5}$, PM_{10}, SO_2, NO_2, O_3, and CO within the whole investigation period. Within 4 years sampling (2014–2017) annual mean figures of $PM_{2.5}$ and PM_{10} concentration exceeded the set standards of the Class 2 limits of GB3095-2012 (35 and 70 μg/m³, respectively) and guidelines of WHO (10 and 20 μg/m³, respectively). Annual mean figures of $PM_{2.5}$, PM_{10} concentrations, which were 53.2 ± 26.91 and 124.54 ± 82.33 μg/m³, respectively, for CNAAQS Class 2 were higher, than the set ones, by 1.4–1.6 times for $PM_{2.5}$ and by 1.67–1.88 times for PM_{10}, and for WHO by 5–5.7 times for $PM_{2.5}$ and by 5.85–6.6 times for PM_{10}. However, daily mean concentrations of $PM_{2.5}$ and PM_{10} varied in a large range of values between 12 and 327 and 23–1344 μg/m³, where the maximum daily values of PM were at the time of intensive dust storms. Thus, concentrations of $PM_{2.5}$ and PM_{10} were the highest of all pollutants and out of 1460 days of sampling their daily mean concentrations exceeded the set norms of CNAAQS in 1102 days (75.53%) for $PM_{2.5}$ and in 1238 days (84.85%) for PM_{10}. However, subject to WHO guidelines, over-limits for $PM_{2.5}$ and PM_{10} were in 1460 (100%) days of sampling.

Daily mean concentrations of SO_2 varied in the range from 4 to 80 μg/m³; however, annual mean figures did not exceed standards of CNAAQS (60 μg/m³) and were 21.5 ± 14 μg/m³, and only in 20 days of sampling (1.37%) they observed levels of pollution, exceeding the norms. Annual mean values of CO and O_3 also did not exceed the set standards (4 mg/m³ and 160 μg/m³, respectively) and were 1.33 ± 0.72 mg/m³ and 87.13 ± 34.95 μg/m³, daily mean values were in the range of 0.4–4.7 mg/m³ and 18–197 μg/m³ with the levels, exceeding the daily mean values within 6 (0.41%) and 61 (4.18%) days, respectively. Annual mean concentrations of NO_2 were 51.69 ± 21.52 μg/m³, which, by 11.69 μg/m³ exceeds the set standards for this pollutant (40 μg/m³), daily values of NO_2 ranged from 12 to 146 μg/m³ at the level of polluted days of 66.75% (974 days).

To study interannual variability, annual mean values of $PM_{2.5}$ and PM_{10} concentrations were calculated, which show

Table 1 Daily mean seasonal concentrations of principal air pollutants, atmosphere parameters and meteorological factors in the period of 2014–2017

	PM$_{2.5}$ (µg/m³)			PM$_{10}$ (µg/m³)			SO$_2$ (µg/m³)			NO$_2$ (µg/m³)			CO (mg/m³)			O$_3$ (µg/m³)		
	Min	Max	Mean	Min	Max	Mean	Min	Max	Mean	Min	Max	Mean	Min	Max	Mean	Min	Max	Mean
January	12	327	72.12±39.23	39	1344	146±126.26	16	75	39.82±12.83	18	137	59.2±23.13	0.7	4.2	2.11±0.81	26	129	56.45±15.64
February	17	160	61.1±22.12	46	551	131.87±74.43	10	54	26.84±10.07	12	102	48±20.92	0.5	3.1	1.6±0.62	43	140	77.01±18.04
March	27	87	49.99±13.63	50	360	140.11±58.40	7	53	19.5±8.8	17	88	49.07±14.62	0.5	2.2	1.19±0.35	32	142	87.45±22.82
April	20	158	47.3±22.08	42	655	135.22±96.12	4	47	16.52±9.8	20	81	47.8±13.58	0.4	1.9	0.94±0.31	38	185	100.9±31.18
May	20	203	49.69±24.78	26	758	136.41±98.92	4	45	15.6±9.6	16	79	46.61±14.52	0.4	2	0.87±0.32	55	184	114.5±28.26
June	17	85	41.78±12.33	42	248	97.36±33.05	4	36	12.4±6.38	16	79	43.62±13.45	0.4	1.9	0.89±0.25	51	188	122.2±33.69
July	14	89	38.22±10.92	27	184	88.08±26.21	4	24	11.08±4.94	18	70	42.1±12.28	0.5	1.7	0.93±0.23	36	197	111.9±42.13
August	17	97	36±11.87	21	244	84.86±31.40	4	28	12±5.4	16	76	40.16±12.64	0.4	1.8	0.92±0.23	33	192	104.6±32.55
September	21	88	40.7±10.79	32	187	92.27±28.28	5	34	13.23±5.19	18	83	47.01±14.76	0.4	1.8	1±0.26	40	182	95.23±33.07
October	13	100	45.59±14.87	23	267	102.09±37.7	4	33	16.47±5.97	12	88	47.51±16.93	0.4	2	1.14±0.35	24	149	72.49±20.82
November	22	222	71.59±30.7	42	1199	165.95±119.6	11	57	31.81±9.91	24	129	69.44±25.21	0.6	3.4	1.92±0.67	19	114	55.25±17.96
December	24	157	85.26±31.32	35	733	174.27±90.9	15	80	42.68±14.04	24	146	79.79±28.42	0.7	4.7	2.49±0.82	18	99	47.41±14.77
Average	18.6	147.7	53.2±26.91	35.41	560.8	124.54±82.33	7.33	47.16	21.5±14	17.58	96.5	51.69±21.52	0.49	2.55	1.33±0.72	34.5	158.4	87.13±34.95

	AE			AOD			WS (m/s)			T (°C)			V (km)			RH (%)		
	Min	Max	Mean	Min	Max	Mean	Min	Max	Mean	Min	Max	Mean	Min	Max	Mean	Min	Max	Mean
January	0.124	1.564	1.215±0.337	0.021	0.634	0.148±0.101	0.83	4.4	2.37±0.64	−18	1	−6.78±3.35	3	10	6.79±1.25	20	85	48.46±12.81
February	0.073	1.8	1.253±0.386	0.018	0.592	0.153±0.125	1.38	4.4	2.51±0.65	−11	3	−3.78±3.75	3	26	7.36±2.51	23	84	54.78±15.64
March	0.003	1.65	1.141±0.439	0.031	0.655	0.203±0.143	0.83	5.27	2.63±0.9	−7	14	3.14±4.04	5	19	8.19±1.88	22	88	45.41±15
April	0.099	1.531	1.270±0.315	0.053	1.954	0.207±0.156	1.38	6.66	2.77±0.80	3	16	9.05±3.04	3	12	8.61±1.76	20	87	51.97±16.46
May	0.752	1.583	1.339±0.188	0.053	0.839	0.201±0.123	1.38	6.38	2.71±0.85	3	20	13.17±3.62	3	13	8.97±1.64	18	86	47.19±14.55
June	0.13	1.552	1.296±0.269	0.072	1.121	0.210±0.147	1.38	3.88	2.27±0.67	11	23	17.4±2.32	6	10	9.36±1	27	87	56.05±13.93
July	1.056	1.799	1.425±0.105	0.064	0.507	0.159±0.067	0.83	5	2.25±0.63	14	26	19.85±2.75	4	17	9.41±1.21	34	92	60.62±13.51
August	0.638	1.714	1.405±0.163	0.054	0.563	0.2±0.091	0.83	5	2.19±0.66	12	26	18.45±3.2	4	11	9.14±1.33	39	98	64.54±14.71
September	0.75	1.5	1.427±0.127	0.046	0.582	0.166±0.099	0.55	3.88	2.05±0.68	8	20	14.21±2.32	2	10	8.90±1.45	41	90	69.37±10.43
October	0.481	1.516	1.377±0.211	0.052	0.425	0.145±0.076	0.83	4.4	2.27±0.71	−1	16	8.18±3.6	3	11	7.92±1.73	29	96	67.97±14.59
November	0.036	1.5	1.314±0.266	0.037	0.895	0.138±0.112	0.83	3.88	2.13±0.67	−7	7	0.76±3.42	3	10	6.85±1.71	43	88	63.35±11.07
December	0.087	1.527	1.322±0.322	0.031	0.762	0.112±0.10	1.38	3.88	2.33±0.63	−12	1	−5.96±2.63	4	19	6.58±1.73	37	83	58.17±9.56
Average	0.352	1.603	1.315±0.288	0.044	0.794	0.17±0.129	1.03	4.75	2.37±0.72	−0.41	14.4	7.9±9.78	3.58	14	8.17±1.91	29.4	88.66	57.32±15.69

Fig. 2 The city-wide average annual and daily concentrations of $PM_{2.5}$, PM_{10}, SO_2, NO_2, O_3, and CO in Lanzhou during the study period. Error bars indicate standard deviation of the year's mean values
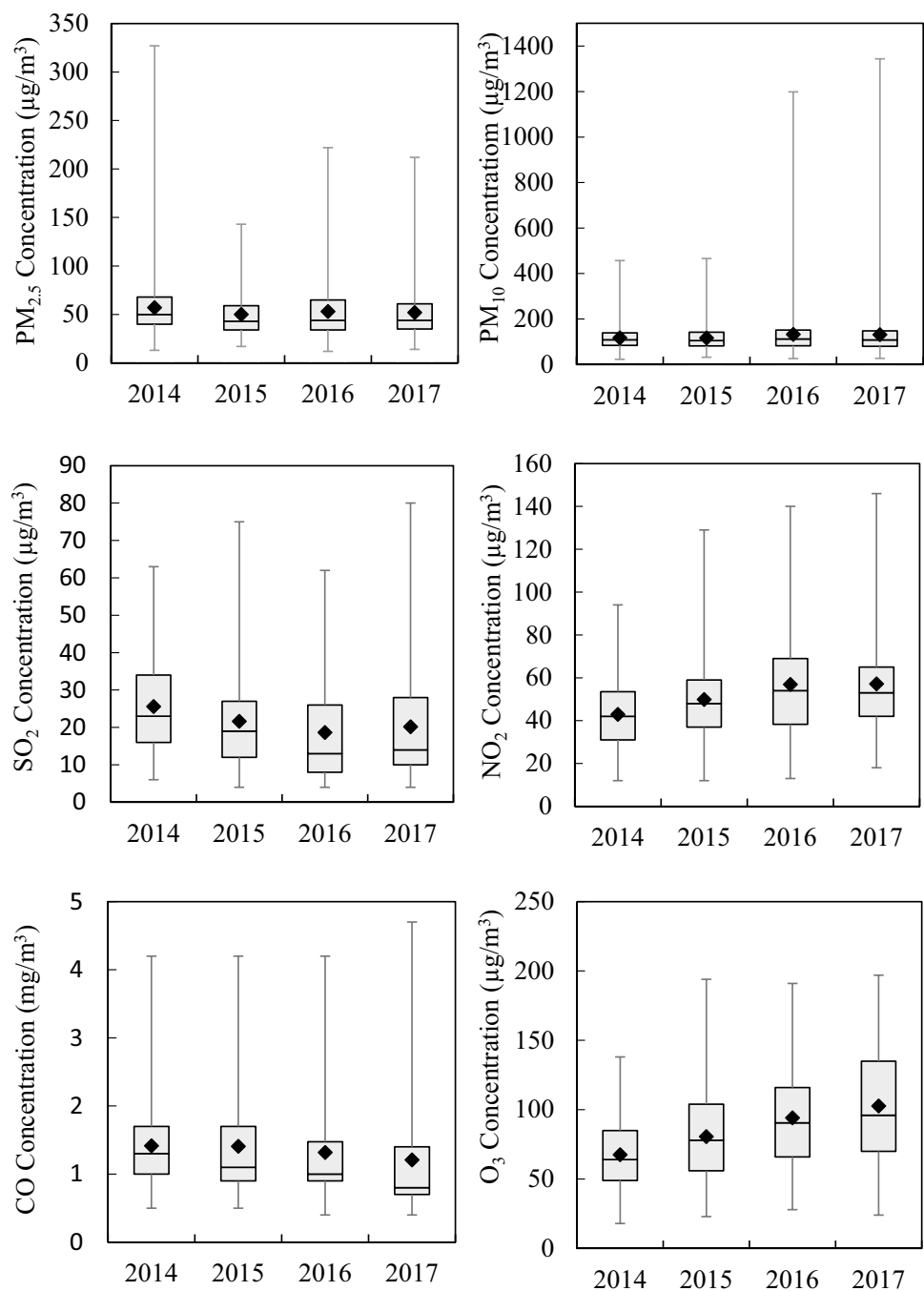
"saw tooth" pattern (permanent alternation between ups and downs) with gradual reduction of $PM_{2.5}$ concentrations from 57.26 ± 27.92 μg/m³ in 2014 to 52.05 ± 26.99 μg/m³ in 2017; however, for PM_{10} increase of the total concentration from 117.29 ± 53.19 μg/m³ in 2014 to 131.42 ± 80.54 μg/m³ in 2017 was observed. Also there were gradual reductions of SO_2 and CO concentrations, annual mean concentrations of SO_2 reduced from 25.58 ± 12.31 μg/m³ in 2014 to 18.65 ± 12.12 μg/m³ in 2016, and then increased to 20.15 ± 15.56 μg/m³ in 2017. CO concentrations had a

tendency to continuously reduce, thus, over four years there was a reduction of CO concentration by 0.21 mg/m³ from value 1.41 ± 0.58 mg/m³ in 2014 to 1.2 ± 0.78 mg/m³ in 2017. However, concentrations of NO_2 and O_3 in the city atmosphere grew steadily year by year. Thus, the level of NO_2 concentration increased from 42.91 ± 15.79 μg/m³ in 2014 to 57.12 ± 21.71 μg/m³ in 2017, the content of ozone in the air basin of the city considerably increased as well from 67.53 ± 24.13 μg/m³ in 2014 to 102.72 ± 39.87 μg/m³ in 2017.

High concentrations of NO_2 and $PM_{2.5}$ may be associated with intensive industrial activity and transport emissions, which are the primary sources of pollutants both in the city and in the whole China (Lindner et al. 2013). In Lanzhou, the number of motor vehicles permanently grows (from 804.6 thousands in 2015 to 1.017 millions in 2017) (LSB 2016, 2018), which adversely affects not only the air quality, but the overall ecological state of urban environment. Due to the fact that the city is situated at a very advantageous strategic location, main transportation and trade routes pass through it, also some of the principal chemical and oil refinery enterprises of region are focused in the city, which results in aerosols emissions to the atmosphere. Also the region of the country, where Lanzhou is situated, constantly experiences a large number of sand-storms, especially in spring, which results in a high content of coarse aerosols in atmosphere not only Lanzhou, but many other cities of Northwest China (Xin et al. 2010; Filonchyk et al. 2018).

Annual and daily concentrations of pollutants in the air on 4 locations, situated in the urban area, show that annual mean concentrations of $PM_{2.5}$, PM_{10}, SO_2, NO_2, CO and O_3 within the whole study period varied in the range from 50 ± 23.2 (S4) to 61 ± 27.5 (S1) $\mu g/m^3$, from 115 ± 60.5 (S4) to 132 ± 73.2 (S1) $\mu g/m^3$, from 28 ± 10.3 (S1) to 31 ± 14.8 (S4) $\mu g/m^3$, from 49 ± 16.3 (S3) to 55 ± 18.4 (S1) $\mu g/m^3$, from 1.3 ± 0.38 (S2, S4) to 1.4 ± 0.45 (S1, S3) mg/m^3 and from 83 ± 33.5 (S1) to 92 ± 36.1 (S4) $\mu g/m^3$, respectively.

The highest levels of pollution were observed in S1, located in the industrial center of the city, which is characterized with continuous industrial emissions throughout the year. S2, located in the adjacent district with a transition type of housing from industry to residential quarters, is also characterized with high atmospheric pollution, and under the influence of accompanying winds receives a part of pollutants from the neighboring district (S1). S3 and S4 are located in residential quarters, high concentrations of pollutants are attributed to a large amount of vehicles, from which emissions the city atmosphere gets compromised. Generally, there is no much disarrangement in the levels of substances concentrations between the city stations, which is attributed to the peculiarity of the city development and relief due to which a gradual distribution of pollutants all over the city occurs.

Variation of aerosol optical depth and Ångström exponent

At present, one of efficient means of investigation of aerosol optic properties in the vertical atmosphere column is remote radiometer sounding. Thus, AOD may be measured for evaluation of aerosols loading in the atmosphere, radiation action on atmosphere and climate; and spectral dependence of AOD, which is expressed by Ångström exponent (AE),

and study the relationship between AOD and AE may be useful for different types of aerosols, moreover, it may also provide information on the predominant size of particulate matter (Xin et al. 2007). Generally, AE ranges from 0.0 to 2.0, while the less values of AE correspond to the larger size of aerosol particles, that is values less than 1 are coarse particles, such as coarse dust, and the exponent values larger than 1 indicate the predominance of fine particles (Hsu et al. 2004; Liu et al. 2018).

Table 1 shows annual mean values of AOD and AE based on results of 943 days of sampling in the period 2014–2017. As is seen from the table, there are very wide ranges of AOD values (from 0.018 to 1.954) and AE values (from 0.003 to 1.8). Quadrennial annual mean values for AOD were 0.17 ± 0.129 and for AE—1.315 ± 0.288; however, during the whole study period there was a gradual decrease of AOD values and increase of AE values from 2014 to 2017 (for AOD—0.18 ± 0.152, 0.179 ± 0.141, 0.161 ± 0.112, 0.146 ± 0.124 and for AE – 1.285 ± 0.343, 1.297 ± 0.339, 1.314 ± 0.148, 1.362 ± 0.129, respectively) (Fig. 3). A broad range of AE from less than 0.2 to close to 2.0 suggests the different types of aerosols (from very fine pollution mode to coarse dust). High values of AE prove the fact that aerosol contains a large number of fine-fraction particles of human origin (Gong et al. 2017). Moreover, dust, blown by wind and generated by construction works, vehicles, branches of industry, unfavorable synoptical weather conditions and poor vegetation cover in this region also contributed to a high AOD (Qiu et al. 2016).

Scatter plot, demonstrated in Fig. 4, shows interrelation between AOD and AE. Pattern of distribution between AOD and AE values in this investigation clearly shows the increase of AOD with decrease of AE, which means the presence of coarse particles in atmosphere. It is most likely
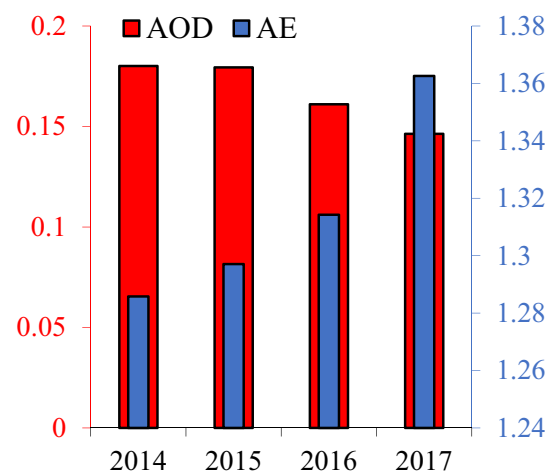

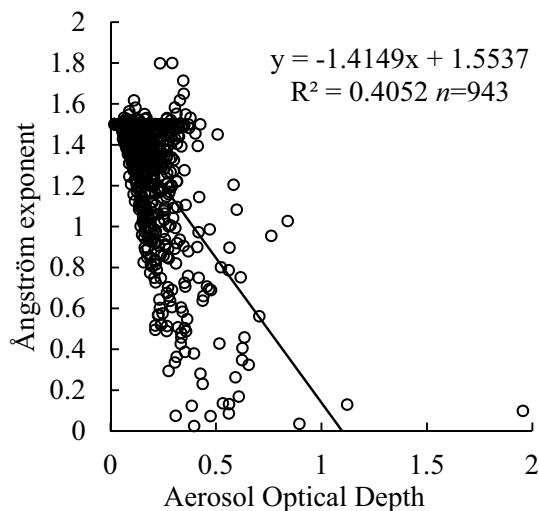**Fig. 3** Interannual variations of aerosol optical depth and Ångström exponent in the city

Fig. 4 Relationship between the Ångström exponent (440/870 nm) and the aerosol optical depth (550 nm) from 2014 to 2017 years

Monthly and seasonal variations in air pollutants and AOD

Based on the data from four states' air quality stations in Lanzhou from 2014 to 2017 (Fig. 1), they got monthly and seasonal levels of concentrations as well as tendencies of variation in particulate matter ($PM_{2.5}$ and PM_{10}) and gas pollutants (SO_2, NO_2, CO and O_3) in the city.

Monthly mean concentrations of $PM_{2.5}$ and PM_{10} (Table 1), respectively, showed the highest concentrations from November to January (71.59 ± 30.7, 85.26 ± 31.32, 72.17 ± 39.23 and 165.95 ± 119.6, 174.27 ± 90.9, 146 ± 126.26 µg/m³, respectively) and the lowest ones in August (36 ± 11.87 and 84.86 ± 31.40 µg/m³). The highest concentrations of SO_2, NO_2 and CO, respectively, 42.68 ± 14.04, 79.79 ± 28.42 µg/m³ and 2.49 ± 0.82 mg/m³ were observed in December, and minimal concentrations for SO_2—in July (11.08 ± 4.94 µg/m³), NO_2—in August (40.16 ± 12.64 µg/m³) and CO—in May (0.87 ± 0.32 mg/m³). The highest concentration of O_3 was in June (122.2 ± 33.69 µg/m³) and the lowest—in December (47.41 ± 14.77 µg/m³). AOD, which is one of the basic atmosphere parameters, shows high values in April and June

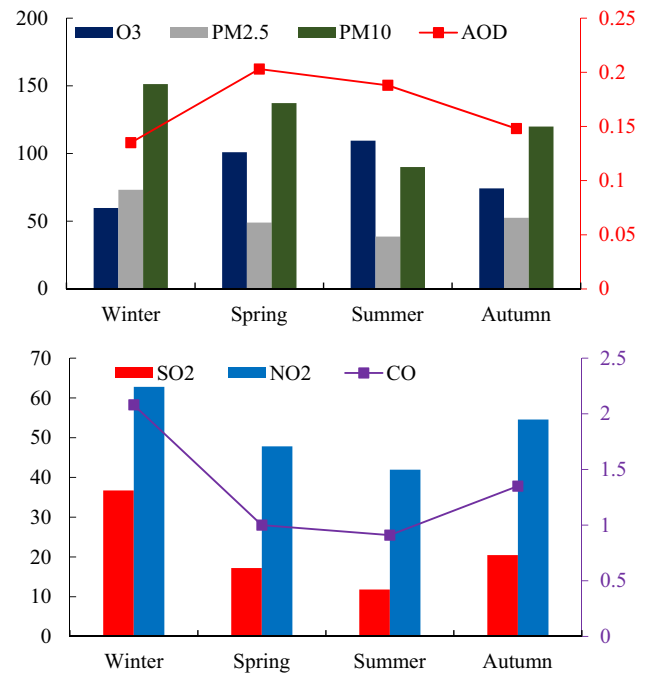that the source of such type of aerosols are local and regional dust events. There are also cases, when AOD is about 0.5 and AE is about 1.0, which reflects the presence of fine particles such as sulphate and black carbon (Che et al. 2013; Liu et al. 2018). In the general case, the relationship between the values of AOD and AE may be clearly described based on equation of linear regression $y = -1.4149x + 1.5537$ where $R^2 = 0.4052$.

Fig. 5 Seasonal variations in air pollutants in Lanzhou during 2014–2017. The units for $PM_{2.5}$, PM_{10}, SO_2, NO_2 and O_3, are µg/m³, whereas that for CO is mg/m³

(0.201 ± 0.156 and 0.210 ± 0.147) and low—in December (0.112 ± 0.10).

Seasonal pollutants variations are shown in Fig. 5. Mean concentration of $PM_{2.5}$ showed a great temporal variability, with the highest value in winter (73.21 ± 33.30 µg/m³) and the lowest—in summer (38.63 ± 11.92 µg/m³)—and in autumn (52.55 ± 24.59 µg/m³) it was a bit higher, than in spring (49.01 ± 20.66 µg/m³). Elevated levels of $PM_{2.5}$ in winter were the result of coal and biomass combustion for residential premises heating (Cheng et al. 2017). Besides, less amount of precipitations, the lower temperature and the height of boundary layer as well as the lighter winds in winter may worsen environmental pollution still greater (Xu et al. 2016a, b). Gradual increase of precipitations by summer season contributes to reduction of concentrations both $PM_{2.5}$, and other pollutants due to fast sedimentation. Besides, low relative humidity, high temperatures and solar radiation may not only prevent removal of fine particles (Bigi and Ghermandi 2011), but also promote their generation (Wu et al. 2008), which results in the growth of PM concentration. Industrial emission sources could play a significant role in accumulation of $PM_{2.5}$ in all seasons due to a great number of plants (Xiao et al. 2018). Besides, biomass combustion also resulted in the increase of $PM_{2.5}$ in spring and autumn (Wang et al. 2014). Seasonal variation of PM_{10} was similar to variation of $PM_{2.5}$ and varied in the order winter→spring→autumn→summer, with maximum

in winter (151.26 ± 101.5 μg/m³), spring (137.28 ± 86.09 μg/m³), autumn (119.55 ± 80.62 μg/m³) to minimum in summer (90.02 ± 30.71 μg/m³). Simultaneous action of industrial sources and unfavorable weather conditions contributed to pollutant accumulation in winter and in spring, which are characterized by a great number of sand-storms from deserts of North and Northwest China, which contribute to high concentrations of coarse aerosols in the city atmosphere (Song et al. 2015).

For NO_2, SO_2, and CO the highest concentrations were registered in winter (62.77 ± 27.7 μg/m³, 36.72 ± 14.19 μg/m³ and 2.08 ± 0.84 mg/m³, respectively), and the lowest—in summer (41.94 ± 12.84 μg/m³, 11.82 ± 5.62 μg/m³ and 0.91 ± 0.24 mg/m³, respectively). Standing meteorological conditions, characterized by feeble winds and poor air displacement in atmosphere layers, which more often occur in winter, catch pollutants near surface and result in their high concentrations (Zhao et al. 2015). Moreover, sources of fossil fuel combustion, such as coal, as well as sulfur-containing fuel, contributed to high pollution generation in winter (Filonchyk and Yan 2018). Solar radiation, strong turbulence currents, increased photochemical activity and a great amount of precipitations resulted in dilution of pollutants near the ground surface, which caused lower concentrations of NO_2, SO_2, and CO in summer (Fan et al. 2014). Taking into account that CO is generated from combustion of biomass, including open burning of straw during crop harvesting, it is the key reason of higher concentration of CO in autumn, than in spring. Nevertheless, concentration of O_3 showed opposite seasonal fluctuations with high value in summer (109.55 ± 36.47 μg/m³) and the lowest value (59.78 ± 20.22 μg/m³) in winter. Faint sunlight in winter may prevent generation of O_3, as the rate of O_3 generation depends on intensity of solar streams.
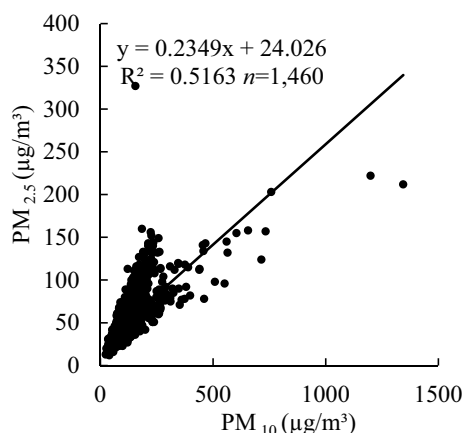

Fig. 6 Density scatter plot of PM_{10} and $PM_{2.5}$ concentrations measured at Lanzhou from 2014 to 2017

Seasonal variations of AOD for the entire study period are shown in Fig. 5. AOD values in Lanzhou show seasonal variation with maximum in spring (0.203 ± 0.176), with gradual reduction in summer (0.188 ± 0.106) and autumn (0.148 ± 0.097) to minimum—in winter (0.135 ± 0.110). High AOD values in spring are attributed to impact of sand and dust, which are generated due to dry climate under the action of arid erosion, which contributes to sand weather (Wang et al. 2017; Sarkar et al. 2018). High AOD values in summer are caused by generation of secondary aerosols due to strong photochemical reactions at high temperature and humidity, which increase aerosols concentrations in atmosphere (He et al. 2016). AOD values are also affected by the peak of biomass combustion in the season of agricultural crop (summer and autumn), which leads to increase in concentration of particles in the air and worsen the air pollution even more (Liu et al. 2018). Another reason associated with air pollution of the city is a specific geography of the locality, resulting in hindered circulation of air flows, which leads to change in weather conditions and amplifies aerosols loading, causing air pollution (Filonchyk et al. 2018).

The relation between PM, AOD and other pollutants

To analyze dependency between concentrations of PM, daily mean values of $PM_{2.5}$ and PM_{10} were used (Fig. 6; Table 3). Upon conducting linear regression from 1460 groups of valid samplings, Pearson correlation coefficient (r) was calculated as 0.719, while R^2 of the regression model reached 0.51 ($p < 0.01$), which emphasizes the significance of correlations between $PM_{2.5}$ and PM_{10} in Lanzhou. Quadrennial monthly mean values of correlation show a wide range of values from 0.44 to 0.954 ($p < 0.01$), provided that the low correlation was in February, and the high correlation—in April (0.938) and May (0.954) ($p < 0.01$), indicating generation of $PM_{2.5}$ and PM_{10} from similar sources. The lower correlation between $PM_{2.5}$ and PM_{10} was observed at increase in mass concentration of PM_{10}, suggesting that fine particles with diameter less than 2.5 μm may not be the only factor, contributing to increase in PM_{10}.

To study relationship between PM, AOD, and AE they used data, obtained based on 943 days of sampling, provided that data on PM were compared with the like data on AOD and AE in the same days during the quadrennial period. For each pair of observation, correlation ratios, presented in Table 2, were calculated. Note that between pairs of $PM_{2.5}$, PM_{10} and AOD, AE there is a good interrelation (between $PM_{2.5}$ and AOD $r = 0.422$, PM_{10} and AOD $r = 0.447$; $PM_{2.5}$ and AE $r = 0.411$, PM_{10} and AE $r = 0.421$) ($p < 0.01$), suggesting a direct dependency between PM and satellite date in the city. It was also found that AOD had no interrelation with AE and consisted $r = -0.637$ ($p < 0.01$). This indicates that increase of AOD over the

Table 2 Pearson's correlation coefficients (r) among environmental variables in Lanzhou 2014–2017

	PM$_{2.5}$ (µg/m³)	PM$_{10}$ (µg/m³)	SO$_2$ (µg/m³)	CO (mg/m³)	NO$_2$ (µg/m³)	O$_3$ (µg/m³)	T (°C)	RH (%)	V (km)	WS (m/s)	AP (mm)	AOD	AE
PM$_{2.5}$ (µg/m³)	1												
PM$_{10}$ (µg/m³)	0.719	1											
SO$_2$ (µg/m³)	0.646	0.327	1										
CO (mg/m³)	0.698	0.299	0.866	1									
NO$_2$ (µg/m³)	0.597	0.358	0.631	0.722	1								
O$_3$ (µg/m³)	−0.339	−0.110	−0.480	−0.480	−0.109	1							
T (°C)	−0.035	0.060	−0.205	−0.080	0.194	0.249	1						
RH (%)	−0.039	0.017	−0.118	−0.154	0.066	0.158	0.029	1					
V (km)	−0.015	0.006	−0.071	−0.007	0.079	0.119	0.507	−0.148	1				
WS (m/s)	−0.028	−0.042	−0.010	0.014	−0.066	−0.051	−0.010	−0.305	0.039	1			
AP (mm)	−0.119	−0.117	−0.15	−0.196	−0.052	0.096	0.198	0.398	0.098	0.111	1		
AOD	0.422	0.447	−0.003	0.005	0.009	−0.089	−0.010	−0.008	−0.001	0.103	−0.101	1	
AE	0.411	0.421	−0.017	0.009	0.051	0.078	0.206	−0.058	0.147	0.010	0.023	−0.637	1

$n=943$ (relationship between PM, AOD, AE, and meteorological parameters); $n=1460$ (relationship between PM and meteorological parameters); $n=1460$ (relationship between PM and gas pollutants); $p<0.01$

Table 3 Correlation between mass concentration of PM$_{2.5}$ and PM$_{10}$

	PM$_{2.5}$/PM$_{10}$ ratio	Correlation coefficients between PM$_{2.5}$ and PM$_{10}$	R^2
January	0.493	0.54	0.29
February	0.463	0.44	0.196
March	0.356	0.722	0.522
April	0.349	0.938	0.881
May	0.364	0.954	0.91
June	0.429	0.684	0.468
July	0.433	0.667	0.445
August	0.424	0.733	0.537
September	0.441	0.76	0.578
October	0.446	0.7	0.491
November	0.431	0.795	0.632
December	0.489	0.622	0.387
Average	0.425	0.712	0.528

$n=1460$; $p<0.01$

study area occurs predominantly with those aerosols with a large size of dust particles, which are transported from deserts of the Central Asia (Filonchyk and Yan 2018).

Pearson correlation coefficients between PM and gas pollutants were calculated based on data of 1460 days of samplings, provided by four monitoring areas. The statistically significant positive pair correlation ($p<0.01$) was found between PM$_{2.5}$, PM$_{10}$, SO$_2$, CO, and NO$_2$, reflecting the similarity of generation of these pollutants (Table 2). Correlation ratios of SO$_2$/CO/NO$_2$ and PM$_{2.5}$ were significantly higher, than ratios of SO$_2$/CO/NO$_2$ and PM$_{10}$, this is attributed to the fact that SO$_2$ and NO$_2$ are essential precursors of SO$_4$ and N O$_3$, respectively, which consist of principal components of PM$_{2.5}$ (Huang et al. 2011). All gaseous pollutants were positively correlated with each other, except for O$_3$, which poorly correlated with other gaseous pollutants. It is attributed to the fact that gaseous pollutants, such as SO$_2$, NO$_2$ and CO as well as aerosol particles, are likely to weaken solar radiation. Generation of O$_3$ was likely in a fair day with high intensity of solar radiation, therefore it showed negative correlation with other pollutants (Chan et al. 2002).

Specific gravity of fine and coarse particles may be evaluated, having studied ratios of PM$_{2.5}$/PM$_{10}$ (Table 3). At quantitative sampling of 1460 days, annual variation of ratios of PM$_{2.5}$/PM$_{10}$ ranged from 0.349 in April to 0.493 in January with the average value 0.425, suggesting that PM$_{10}$ constitutes a considerable proportion in the content of PM in the studied area. High relations of PM$_{2.5}$/PM$_{10}$ are attributed to vehicle emissions and secondary particles, generated in atmosphere from gases (Filonchyk and Yan 2018), while less relations are associated with violent dust emissions from deserts of North and Northwest China in spring, and

repeated suspension due to a large volume of motion (Guan et al. 2017).

The relation between concentrations of PM and meteorological factors

Previous investigations, aimed at atmosphere pollution study, show that atmosphere pollution is caused by both pollutants emissions themselves, and meteorological conditions of the study area (Zhao et al. 2013). When pollutants emissions in city districts are stable, atmosphere pollution is predominantly conditioned by meteorological factors, such as dispersion and wind transportation as well as acceleration of substances leaching by atmospheric precipitations. Besides, photochemical reactions depend on temperature, relative humidity, solar radiation and a number of other conditions. Particles accumulation and transport are closely related to synoptical system and atmospheric circulation (Wu et al. 2013).

Table 1 shows mean values of monthly data for pollutants and meteorological factors. Hourly concentration of pollutants and meteorological parameters first were calculated into daily mean, and then into monthly mean values, which resulted in calculation of correlation ratios. The relation was calculated by Pearson's correlation analysis. As is shown in Table 2, correlation between meteorological conditions and pollutants shows poor positive or negative correlation, indicating slight impact of these parameters on pollutants concentration in atmosphere. It is evident from Table 1 that the range of wind speed in Lanzhou varied from 1.03 to 4.75 m/s, at annual mean wind speed 2.37 m/s, therefore mass concentrations of PM were high throughout all months and varied only slightly with wind speed. There was negative correlation between wind speed and $PM_{2.5}$, PM_{10} with $r = -0.028$, $r = -0.042$ ($p<0.01$), respectively (Table 2). Previous investigations also revealed that the higher levels of PM are associated with the lower wind speed and air temperature (Wu et al. 2013). There is insignificant negative and positive interrelations between temperature and concentrations of PM with $r = -0.035$ and $r = 0.060$ ($p < 0.01$) for $PM_{2.5}$ and PM_{10}, respectively. In particular, high temperature contributes to dispersion of secondary pollutants (Fang et al. 2017), which may be observed in seasonal variation—the higher temperature, the lower PM and other gas pollutants, except for ozone, which concentrations grow subject to temperature rise.

To comprehend the results of investigation and visually understand the interrelation between concentrations of PM and meteorological parameters, frequency histograms for $PM_{2.5}$, PM_{10}, wind speed and temperature were constructed in Fig. 7. Statistics show that during the whole period of time only 357 days for $PM_{2.5}$ and 221 for PM_{10} were characterized by pollution levels, not exceeding CNAAQS, suggesting

that the city is subject to high atmospheric pollution. In this respect, in summer at high temperatures there was the most amount of days with pure air (for $PM_{2.5}$ 157 days and for PM_{10} 95 days), this also proves the fact that high air temperatures obviously contribute to intensive convection, leading to decrease of mass concentrations. In contrast, low temperatures in winter cause radiation cooling, which weakens convection and lead to higher concentrations in this period. Thus, at temperature -6 °C and lower only 31 days for $PM_{2.5}$ and 20 days for PM_{10} were characterized by levels, not exceeding standards. Low wind speeds (2.5–3 m/s), which were predominant during all year seasons, show that feeble wind speeds contribute to accumulation of pollutants in the city atmosphere.

Principal component and cluster analysis

Principal components analysis (PCA) and cluster analysis (CA) were used to reveal possible sources of pollutants emissions and calculate correlations between them. PCA is widely used for reduction of variables number and extraction of a small number of underlying factors for analysis of interrelations between observable variables, which correspond to the same origin or transport route. To make results interpretation easier, they applied PCA with Varimax rotation (Lewis-Beck 1994), which may maximize factor loadings through variables for each factor. Coefficient loadings over 0.71 are usually considered excellent, and less than 0.32—very poor (Nowak 1998). For PCA and CA ten variables were considered, each variable consisted of 1460 samplings.

At PCA with Varimax rotation all principal components with their own values (eigenvalues) > 1 were remained according to Kaiser criterion (Kaiser 1960). PCA identified three factors, to which 67% of the entire set of data was attributed (Table 4). The first factor (F1), consisted of $PM_{2.5}$, PM_{10}, CO, SO_2 and NO_2, to a great degree explains 36% of all data, closely related to vehicle emissions and industrial sources, combustion of fuel for heating (coal, crude oil, timber, biomass), which are likely the primary sources of air pollution in Lanzhou. Linear correlations between $PM_{2.5}$, PM_{10}, CO, SO_2, and NO_2 (Table 2) were also high, which suggests a high interrelation between these pollutants. The second factor (F2), heavily loaded with temperature and visibility, explained 16.94% of all data, and the third factor (F3), consisted of relative humidity, explained 14.11%. This enables to suppose that meteorological parameters are one of key factors of air pollution.

CA is an efficient multivariant statistical approach, which may be used to achieve more confidence in final classification, obtained with PCA. Therefore in this work CA was used for comparison purposes. Dendrogram was obtained based on Ward's method with use of Euclidian distances as a criterion in clusters generation. This CA
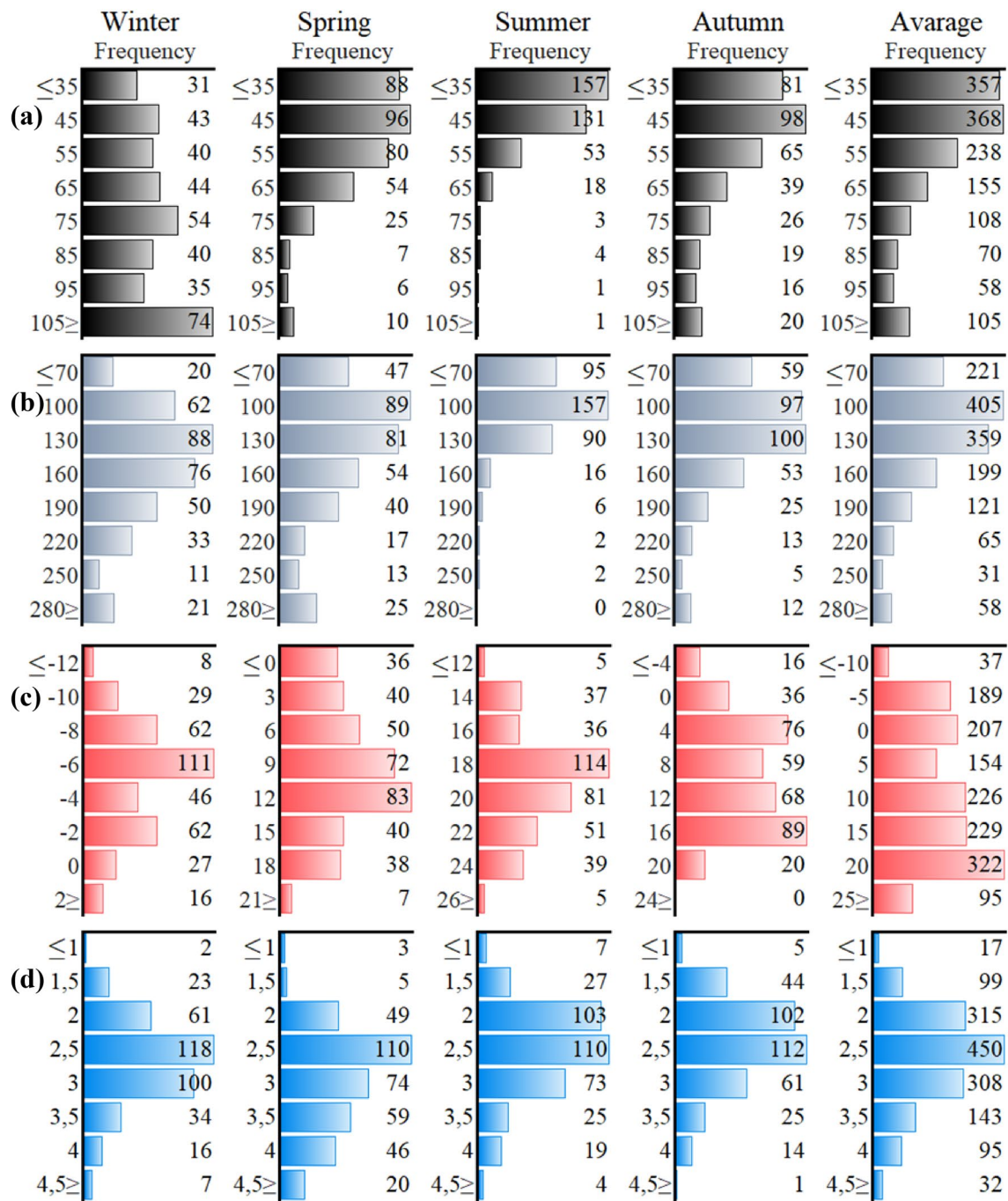
Fig. 7 The frequency histograms of $PM_{2.5}$ (**a**), PM_{10} (**b**), temperature (**c**) and wind speed (**d**) in Lanzhou

form is considered efficient, though it generates, as a rule, small clusters. Results of CA are shown in Fig. 8. By samples of various pollutants and meteorological parameters in Euclidian distance 20 four groups were classified: cluster 1 ($PM_{2.5}$, NO_2, SO_2), cluster 2 (CO), cluster 3 (PM_{10}), and cluster 4 (RH, V, T, O_3, WS). Clusters 1 and 2 in dendrogram were explained by high levels of emissions from transport, biomass combustion, use of sulfur-containing

fuels, which may contribute to high levels of $PM_{2.5}$, NO_2, SO_2, and CO in the city, which corresponds to results, obtained with PCA (Table 4). Cluster 3 implies that in addition to vehicle emissions, PM_{10} may also originate from such sources as building activities in city districts, industry and sand-storms. In the general case, grouping, obtained with CA, is in line with PCA results.

Table 4 The factor loadings after principal component analysis VAR-IMAX rotation at the study area

	F1	F2	F3	F4
$PM_{2.5}$	**0.87**	− 0.12	− 0.08	0.3
PM_{10}	**0.6**	− 0.26	− 0.17	**0.68**
SO_2	**0.88**	0.15	0.03	− 0.21
CO	**0.91**	0.04	0.09	− 0.26
NO_2	**0.76**	− 0.35	− 0.09	− 0.18
O_3	− 0.51	− 0.45	− 0.18	0.22
T	− 0.09	**− 0.84**	0.18	− 0.11
RH	− 0.11	− 0.17	**− 0.78**	− 0.07
V	− 0.04	**− 0.68**	0.42	− 0.20
WS	− 0.01	0.15	**0.7**	0.34
Eigenvalues	3.6	1.68	1.41	0.93
% of variance	36	16.8	14.1	9.3
Cumulative %	36	52.8	67	76.4

Values > 0.6 are significant and are given in bold
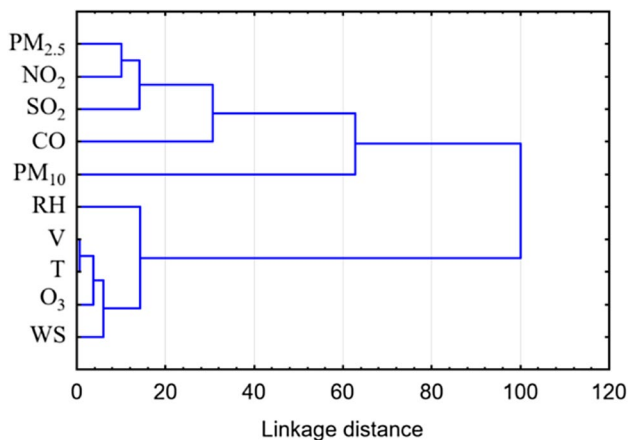
Fig. 8 Dendrogram resulting from the Ward's method of hierarchical cluster analyses

Air mass back trajectory and aerosol vertical distribution

Investigations on nature of air masses movement and principal directions of smoke aerosol and gaseous impurities transportation in the studied area were conducted using trajectory model of reanalysis of the National Oceanic and Atmospheric Administration (NOAA) Air Resources Laboratory's (ARL) Hybrid Single-Particle Lagrangian Integrated Trajectory model (HYSPLIT) (Draxler and Hess 1998; Draxler and Rolph 2013; Stein et al. 2015; Rolph et al. 2017) and archive meteorological data archive Global Data Assimilation System (GDAS). It is to be noted that NOAA HYSPLIT model enables to calculate forward and backward trajectories of air masses movement in the atmospheric boundary layer taking into account vertical transfers.

To run trajectories geographical coordinates of Lanzhou were specified (N36°02′1″ E103°48′4″). Trajectories of air masses movement were calculated for quadrennial period from 2014 to 2017 for 12:00 UTC with duration 72 h at a height of 1000 meters and reflected to the fullest extent long-range pollutants transport at regional and global scales. Totally 730 trajectories for all seasons were run, which are shown in Fig. 9. It has been established that generally northern, north western and western drift of air masses prevails for all study regions. Trajectories, obtained in different seasons, show similar characteristics of air masses movement. It is notable that the general picture of air masses origin, obtained from reconstructed backward trajectories, is virtually unaltered during the period under review. Backward trajectories show that air masses predominantly originate from the Gobi, Gurbantunggut and Taklamakan deserts, which are the main sources of natural dust aerosol, affecting atmosphere not only of China, but the whole Asian continent as well (Filonchyk et al. 2018).

To reveal aerosols types as well as their vertical distribution during large sand-storms near the study area, data from the CALIPSO satellite were used. Figure 10 shows 523 nm total attenuated backscatter coefficient and aerosol subtype during large dust storms on January 26 (ascent orbit at nighttime at 18.58) and on April 17, 2017 (descend orbit during the daytime at 6.00), when concentrations of coarse particles PM_{10} in the air were 1344 and 564 μg/m³. The total attenuated backscatter is one of basic parameters of the CALIPSO satellite, reflecting the capacity of aerosol scattering. Figure 10 shows general tendency of frequency distribution of total attenuated backscatter coefficient of aerosols, vary in height. Results showed that values of total attenuated backscatter coefficient in the entire height profile 0–10 km are focused in the range of 0.0002–0.045 $km^{-1} \times sr^{-1}$. Figure 10 also demonstrates images, showing clear one- and two-layer structures. In addition to local pollution layers, upper layers of pollutants were found at the height of 2–6 km (for January 26, 2017) and 2–5 km (for April 17, 2017). They were classified as dust interspersed with polluted dust. Taking into consideration that nighttime and daytime trajectories of the satellite movement pass over different areas of the territory, on January 26, 2017 the satellite went over the territory of the Gobi Desert and Ningxia and the South part of Gansu province, and on April 17, 2017, through the North of Xinjiang, Taklamakan Desert, a part of the Tibetan Plateau and the east of Qinghai Province, where strong aerosol horizons were found on the ground and on high altitudes.

Thus, based on the backward trajectories and data from the CALIPSO satellite, the spring and winter heavy haze is predominantly caused by dust formation, and PM_{10} is the
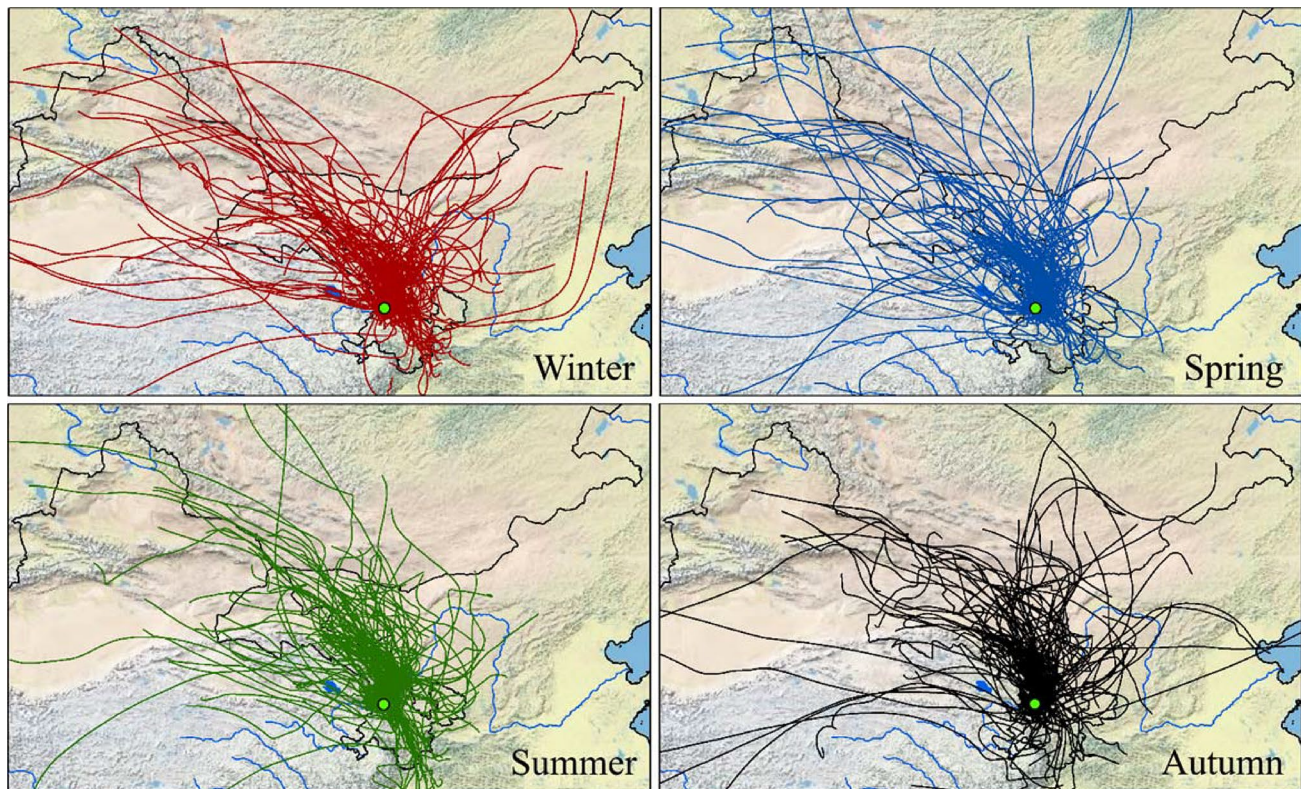
Fig. 9 72-h backward trajectories of air masses arriving in Lanzhou every 12 h at 1000 m during the dust event period

principal pollutant. Besides, the air quality worsens due to dry weather and relative high wind speed, which contributes to dust emission through arid erosion and its transportation to the studied area.

Conclusion

Based on data on principal atmospheric pollutants in the city of Lanzhou obtained for the quadrennial period from 2014 to 2017 from ground-based air quality stations, located in the urban area, as well as satellite data, the following conclusions were drawn:

Heavy air pollution was predominantly caused by high concentrations of $PM_{2.5}$ and PM_{10}. Annual mean concentrations of $PM_{2.5}$ and PM_{10}, obtained based on data of 1460 days of samplings, were 53.2 ± 26.91 and 124.54 ± 82.33 µg/m^3, respectively. Daily mean concentrations of $PM_{2.5}$ exceeded the set norms of CNAAQS in 1102 days (75.53%) and PM_{10} in 1238 days (84.85%) of the total days of investigation. However, subject to WHO guidelines, over-limits for $PM_{2.5}$ and PM_{10} reached 1460 (100%) days. $PM_{2.5}$, PM_{10}, NO_2, SO_2, and CO showed the highest levels in winter and the lowest—in summer, suggesting cumulative action of industrial sources and unfavorable weather conditions on

dilution of air pollution and dispersion. Nevertheless, concentration of O_3 peaked in summer, which was associated with heavy solar irradiation.

Data, obtained with the MODIS satellite, shows broad ranges for AOD (from 0.018 to 1.954) and AE values (from 0.003 to 1.8). However, annual mean values for AOD were 0.17 ± 0.129 and for AE, 1.315 ± 0.288, while there was a gradual decrease of AOD values and increase of AE values for the whole study period with values (for AOD— 0.18 ± 0.152, 0.179 ± 0.141, 0.161 ± 0.112, 0.146 ± 0.124; and for AE—1.285 ± 0.343, 1.297 ± 0.339, 1.314 ± 0.148, 1.362 ± 0.129), respectively, in the period from 2014 to 2017. However, there is a relationship between AOD, AE and PM values, suggesting a strong relationship between the pairs of $PM_{2.5}$, PM_{10}, and AOD, AE (between $PM_{2.5}$ and AOD $r = 0.422$, PM_{10} and AOD $r = 0.447$; $PM_{2.5}$ and AE $r = 0.411$, PM_{10} and AE $r = 0.421$) ($p < 0.01$).

PCA and CA were used to identify possible sources of pollutants emissions. PCA identified three factors, to which 67% of the total set of data was attributed. F1 consisted of $PM_{2.5}$, PM_{10}, CO, SO_2, and NO_2 and explained 36% of total data. F2 was heavily loaded with temperature and visibility and explained 16.94% of all data, and F3 consisted of relative humidity and explained 14.11%. Results of CA by samples of various pollutants and meteorological parameters
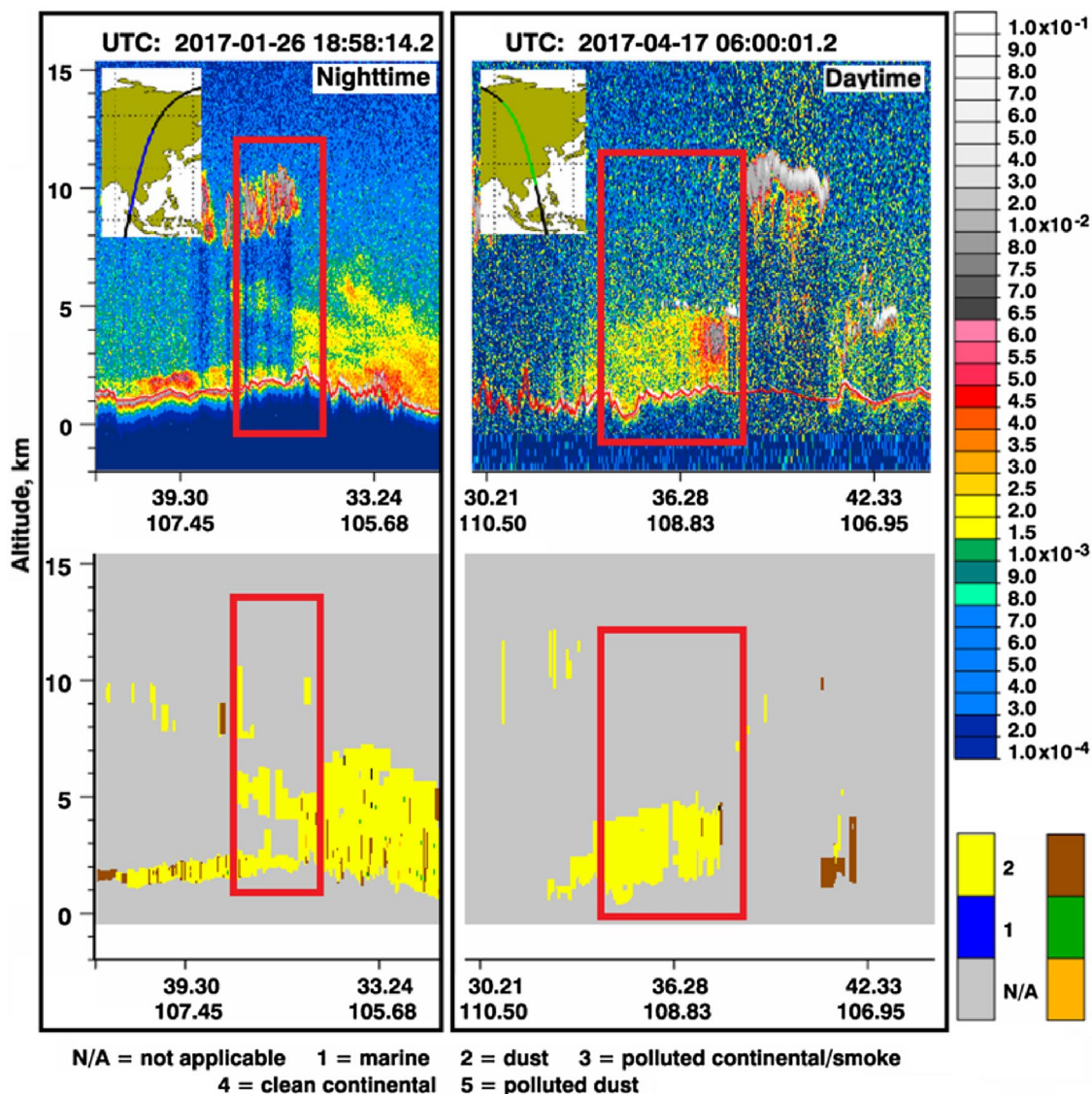
Fig. 10 CALIPSO 523 nm total attenuated backscatter coefficient and aerosol subtype on January 26 and April 17, 2017 in Lanzhou. The monitoring area is specified in the red square

were classified by four groups: cluster 1 ($PM_{2.5}$, NO_2, SO_2), cluster 2 (CO), cluster 3 (PM_{10}) and cluster 4 (RH, V, T, O_3, WS). Clusters 1 and 2 are explained by high levels of emissions from transport, biomass combustion, use of sulfur-containing fuels. Cluster 3 implies that in addition to vehicle emissions, PM_{10} may also originate from such sources as building activities and sand-storms.

This investigation is aimed at the study of characteristics of six principal atmospheric pollutants in the city of Lanzhou, aerosols properties as well as understanding of relationship between pollutants and meteorological factors, which may facilitate not only more effective evaluation of air quality, climate and weather change, but also play an important role in the research in the field of ecology, health care and epidemiology and give recommendations on the public policy development, aimed at the control over emissions in China. In the future, investigations should be focused on more detailed observations of both concentrations of six principal atmospheric pollutants, and chemical constituents from industrial, residential, and suburban areas of the city.

References

Bigi A, Ghermandi G (2011) Particle number size distribution and weight concentration of background urban aerosol in a Po Valley site. Water Air Soil Pollut 220(1–4):265–278

Cao X, Wang Z, Tian P, Wang J, Zhang L, Quan X (2013) Statistics of aerosol extinction coefficient profiles and optical depth using lidar measurement over Lanzhou, China since 2005–2008. J Quant Spectrosc Radiat Transfer 122:150–154

Chan CY, Chan LY, Lam KS, Li YS, Harris JM, Oltmans SJ (2002) Effects of Asian air pollution transport and photochemistry on carbon monoxide variability and ozone production in subtropical coastal south China. J Geophys Res 107(D24):4746

Che H, Wang Y, Sun J, Zhang X, Zhang X, Guo J (2013) Variation of aerosol optical properties over the Taklimakan Desert in China. Aerosol Air Qual Res 13:777–785

Chen P, Wang T, Dong M, Kasoar M, Han Y, Xie M, Huang T (2017) Characterization of major natural and anthropogenic source profiles for size-fractionated PM in Yangtze River Delta. Sci Total Environ 598:135–145

Cheng Y, He KB, Engling G, Weber R, Liu JM, Du ZY, Dong SP (2017) Brown and black carbon in Beijing aerosol: implications for the effects of brown coating on light absorption by black carbon. Sci Total Environ 599:1047–1055

Costa DL, Dreher KL (1997) Bioavailable transition metals in particulate matter mediate cardiopulmonary injury in healthy and compromised animal models. Environ Health Perspect 105(5):1053–1060

Draxler RR, Hess GD (1998) An overview of the HYSPLIT_4 modelling system for trajectories. Aust Meteorol Mag 47(4):295–308

Draxler RR, Rolph GD (2013) HYSPLIT (HYbrid single-particle lagrangian integrated trajectory) model access via NOAA ARL READY website. NOAA Air Resources Laboratory, College Park. http://www.arl.noaa.gov/HYSPLIT.php. Accessed 29 Oct 2013

Fan J, Yue X, Jing Y, Chen Q, Wang S (2014) Online monitoring of water-soluble ionic composition of PM10 during early summer over Lanzhou City. J Environ Sci 26(2):353–361

Fang C, Zhang Z, Jin M, Zou P, Wang J (2017) Pollution characteristics of PM2.5 aerosol during haze periods in Changchun, China. Aerosol Air Qual Res 17:888–895

Filonchyk M, Yan H (2018) Urban air pollution monitoring by ground-based stations and satellite data: multi-season characteristics from Lanzhou City, China. Springer, Berlin

Filonchyk M, Yan H, Yang S, Hurynovich V (2016) A study of PM2.5 and PM10 concentrations in the atmosphere of large cities in Gansu Province, China, in summer period. J Earth Syst Sci 125(6):1175–1187

Filonchyk M, Yan H, Li X (2018) Temporal and spatial variation of particulate matter and its correlation with other criteria of air pollutants in Lanzhou, China, in spring-summer periods. Atmos Pollut Res. https://doi.org/10.1016/j.apr.2018.04.011

Gong C, Xin J, Wang S, Wang Y, Zhang T (2017) Anthropogenic aerosol optical and radiative properties in the typical urban/suburban regions in China. Atmos Res 197:177–187

Guan Q, Cai A, Wang F, Yang L, Xu C, Liu Z (2017) Spatio-temporal variability of particulate matter in the key part of Gansu Province, Western China. Environ Pollut 230:189–198

Hagler GSW, Bergin MH, Salmon LG, Yu JZ, Wan ECH, Zheng M, Schauer JJ (2006) Source areas and chemical composition of fine particulate matter in the Pearl River Delta region of China. Atmos Environ 40(20):3802–3815

He Q, Zhou G, Geng F, Gao W, Yu W (2016) Spatial distribution of aerosol hygroscopicity and its effect on PM2.5 retrieval in East China. Atmos Res 170:161–167

Hsu NC, Tsay SC, King MD, Herman JR (2004) Aerosol properties over bright-reflecting source regions. IEEE Trans Geosci Remote Sens 42(3):557–569

Hu J, Wang Y, Ying Q, Zhang H (2014) Spatial and temporal variability of PM2.5 and PM10 over the North China Plain and the Yangtze River Delta, China. Atmos Environ 95:598–609

Huang K, Zhuang G, Lin Y, Fu J, Wang Q, Liu T, Zhang R, Jiang Y, Deng C (2011) Typical types and formation mechanisms of haze in an eastern Asia megacity, Shanghai. Atmos Chem Phys Dis 11(8):21713–21767

Kaiser HF (1960) The application of electronic computers to factor analysis. Educ Psychol Meas 20:141–151

Kong L, Xin J, Zhang W, Wang Y (2016) The empirical correlations between PM2.5, PM10 and AOD in the Beijing metropolitan region and the PM2.5, PM10 distributions retrieved by MODIS. Environ Pollut 216:350–360

Lewis-Beck MS (1994) Factor analysis and related techniques. Sae and Toppan Publications, USA

Lindner S, Liu Z, Guan D, Geng Y, Li X (2013) CO2 emissions from China's power sector at the provincial level: consumption versus production perspectives. Renew Sust Energ Rev 19:164–172

Liu W, Zhang HR, Yan DP, Wang SL (2017) Adaptive surface modeling of soil properties in complex landforms. ISPRS Int J Geo Inf 6(6):178

Liu C, Chung CE, Yin Y, Schnaiter M (2018) The absorption Ångström exponent of black carbon: from numerical aspects. Atmos Chem Phys 18(9):6259–6273

LSB (Lanzhou Statistical Bureau) (2016) Lanzhou statistical yearbook. China Statistics Press, China, Beijing

LSB (Lanzhou Statistical Bureau) (2018) Lanzhou statistical yearbook. China Statistics Press, China, Beijing

Lv B, Liu Y, Yu P, Zhang B, Bai Y (2015) Characterizations of PM2.5 pollution pathways and sources analysis in four large cities in China. Aerosol Air Qual Res 15(5):1836–1843

MEP (Ministry of Environmental Protection of the People's Republic of China) (2012) China national ambient air quality standards. Ministry of Environmental Protection, China, Beijing

MEP (Ministry of Environmental Protection of the People's Republic of China) (2013a) National standards on environmental protection: technical specifications for installation and acceptance of ambient air quality continuous automated monitoring system for PM10 and PM2.5 (HJ655–2013). Ministry of Environmental Protection, China, Beijing

MEP (Ministry of Environmental Protection of the People's Republic of China) (2013b) National standards on environmental protection: technical specifications for installation and acceptance of ambient air quality continuous automated monitoring system for SO2, NO2, O3 and CO (HJ193–2013). Ministry of Environmental Protection, China, Beijing

Na L, Ye Y, He J, Zhao S (2013) Integrated modeling of urban-scale pollutant transport: application in a semi-arid urban valley, northwestern china. Atmos Pollut Res 4(3):306–314

Nowak B (1998) Contents and relationship of elements in human hair for a non-industrialised population in Poland. Sci Total Environ 209(1):59–68

Pan G, Zhang S, Feng Y, Takahashi K, Kagawa J, Yu L (2010) Air pollution and children's respiratory symptoms in six cities of northern China. Respir Med 104(12):1903–1911

Qiu X, Duan L, Gao J, Wang S, Chai F, Hu J, Yun Y (2016) Chemical composition and source apportionment of PM10 and PM2.5 in different functional areas of Lanzhou, China. J Environ Sci 40:75–83

Remer LA, Kaufman YJ, Tanré D, Mattoo S, Chu DA, Martins JV, Eck TF (2005) The MODIS aerosol algorithm, products, and validation. J Atmos Sci 62(4):947–973

Remer LA, Mattoo S, Levy RC, Munchak LA (2013) MODIS 3 km aerosol product: algorithm and global perspective. Atmos Meas Tech 6:1829–1844

Rolph G, Stein A, Stunder B (2017) Real-time environmental applications and display sYstem: READY. Environ Model Softw 95:210–228

Sarkar T, Mishra M (2018) Soil erosion susceptibility mapping with the application of logistic regression and artificial neural network. J Geovis Spat Anal 2(1):8

Sayer AM, Munchak LA, Hsu NC, Levy RC, Bettenhausen C, Jeong MJ (2014) MODIS Collection 6 aerosol products: comparison between aqua's e-deep blue, dark target, and "merged" data sets, and usage recommendations. J Geophys Res Atmos 119(24):13965–13989

Song X, Shao L, Zheng Q, Yang S (2015) Characterization of crystalline secondary particles and elemental composition in PM10, of North China. Environ Earth Sci 74(7):5717–5727

Stein AF, Draxler RR, Rolph GD, Stunder BJ, Cohen MD, Ngan F (2015) NOAA's HYSPLIT atmospheric transport and dispersion modeling system. Bull Am Meteor Soc 96(12):2059–2077

Tan J, Xiang P, Zhou X, Duan J, Ma Y, He K, Querol X (2016) Chemical characterization of humic-like substances (HULIS) in PM2.5 in Lanzhou, China. Sci Total Environ 573:1481–1490

Tao Y, Mi S, Zhou S, Wang S, Xie X (2014) Air pollution and hospital admissions for respiratory diseases in Lanzhou, China. Environ Pollut 185:196–201

Tsai TC, Jeng YJ, Chu DA, Chen JP, Chang SC (2011) Analysis of the relationship between MODIS aerosol optical depth and particulate matter from 2006 to 2008. Atmos Environ 45(27):4777–4788

Wang S, Feng X, Zeng X, Ma Y, Shang K (2009) A study on variations of concentrations of particulate matter with different sizes in Lanzhou, China. Atmos Environ 43(17):2823–2828

Wang J, Hu Z, Chen Y, Chen Z, Xu S (2013) Contamination characteristics and possible sources of PM10 and PM2.5 in different functional areas of Shanghai, China. Atmos Environ 68:221–229

Wang Y, Ying Q, Hu J, Zhang H (2014) Spatial and temporal variations of six criteria air pollutants in 31 provincial capital cities in China during 2013–2014. Environ Int 73(1):413–422

Wang X, Cheng H, Che H, Sun J, Lu H, Qiang M, Lang L (2017) Modern dust aerosol availability in northwestern China. Sci Rep 7(1):8741

Winker DM, Vaughan MA, Omar A, Hu Y, Powell KA, Liu Z, Young SA (2009) Overview of the CALIPSO mission and CALIOP data processing algorithms. J Atmos Ocean Technol 26(11):2310–2323

WHO (World Health Organization) (2005) World health organization air quality guidelines global update. In: Report on a working group meeting, Bonn, Germany, 18–20 October 2005, WHO Regional Office for Europe E87950, report

Winker DM, Pelon J, Coakley JA Jr, Ackerman SA, Charlson RJ, Colarco PR, Kubar TL (2010) The CALIPSO mission: a global 3D view of aerosols and clouds. Bull Am Meteor Soc 91(9):1211–1230

Wu Z, Hu M, Lin P, Liu S, Wehner B, Wiedensohler A (2008) Particle number size distribution in the urban atmosphere of Beijing, China. Atmos Environ 42(34):7967–7980

Wu DL, Lin M, Chan CY, Li WZ, Tao J, Li YP, Bu CW (2013) Influences of commuting mode, air conditioning mode and

meteorological parameters on fine particle (PM2.5) exposure levels in traffic microenvironments. Aerosol Air Qual Res 13:709–720

Xia X, Zhang A, Liang S, Qi Q, Jiang L, Ye Y (2017) The association between air pollution and population health risk for respiratory infection: a case study of Shenzhen, China. Int J Environ Res Public Health 14(9):950

Xiao K, Wang Y, Wu G, Fu B, Zhu Y (2018) Spatiotemporal characteristics of air pollutants (PM10, PM2.5, SO2, NO2, O3, and CO) in the Inland Basin City of Chengdu, Southwest China. Atmosphere 9(2):74

Xin J, Wang Y, Li Z, Wang P, Hao WM, Nordgren BL, Sun Y (2007) Aerosol optical depth (AOD) and Ångström exponent of aerosols observed by the Chinese Sun Hazemeter Network from August 2004 to September 2005. J Geophys Res Atmos 112:D5

Xin J, Du W, Wang Y, Gao Q, Li Z, Wang M (2010) Aerosol optical properties affected by a strong dust storm over central and northern China. Adv Atmos Sci 27(3):562–574

Xu Q, Li X, Wang S, Wang C, Huang F, Gao Q, Guo X (2016a) Fine particulate air pollution and hospital emergency room visits for respiratory disease in urban areas in Beijing, China, in 2013. PLoS One 11(4):e0153099

Xu W, Wu Q, Liu X, Tang A, Dore AJ, Heal MR (2016b) Characteristics of ammonia, acid gases, and PM2.5 for three typical land-use types in the NCP. Environ Sci Pollut Res 23:1158–1172

Xu A, Mu Z, Jiang B, Wang W, Yu H, Zhang L (2017) Acute effects of particulate air pollution on ischemic heart disease hospitalizations in Shanghai, China. Int J Environ Res Public Health 14(2):168

Yan D, Lei Y, Shi Y, Zhu Q, Li L, Zhang Z (2018) Evolution of the spatiotemporal pattern of PM2.5 concentrations in China—a case study from the Beijing–Tianjin–Hebei region. Atmos Environ 183:225–233

Zhang YL, Cao F (2015) Fine particulate matter (PM 2.5) in China at a city level. Sci Rep 5:14884

Zhao JG, Wang SG, Wang JY, Jian-Rong BI, Shi JS, Wang TH (2013) Analysis of the relationship between pollution in Lanzhou city and ground meteorological factors. J Lanzhou Univ 49(4):491–490 **(in Chinese)**.

Zhao M, Huang Z, Qiao T, Zhang Y, Xiu G, Yu J (2015) Chemical characterization, the transport pathways and potential sources of PM2.5 in Shanghai: seasonal variations. Atmos Res 158:66–78

Zheng S, Pozzer A, Cao CX, Lelieveld J (2015) Long-term (2001–2012) concentrations of fine particulate matter (PM 2.5) and the impact on human health in Beijing, China. Atmos Chem Phys 15(10):5715–5725

Zheng S, Zhou X, Singh R, Wu Y, Ye Y, Wu C (2017) The spatiotemporal distribution of air pollutants and their relationship with land-use patterns in Hangzhou city, China. Atmosphere 8(6):110

Zhou T, Sun J, Yu H (2017) Temporal and spatial patterns of china's main air pollutants: years 2014 and 2015. Atmosphere 8(8):137